Appl. Phys. A (2014) 116:1085–1089
DOI 10.1007/s00339-013-8190-5

Applied Physics A
Materials Science & Processing

Highly luminescent undoped and Mn-doped ZnS nanoparticles by liquid phase pulsed laser ablation

P. M. Aneesh · M. R. Shijeesh · Arun Aravind · M. K. Jayaraj

Received: 16 July 2013 / Accepted: 3 December 2013 / Published online: 12 December 2013

Abstract In this paper we report the synthesis of highly luminescent ZnS and Mn-doped ZnS nanoparticles with uniform particle size distribution by liquid phase pulsed laser ablation. The formation of nanosized ZnS crystallites was confirmed by high-resolution transmission electron microscopy (HRTEM) images. The optical properties of these nanoparticles were studied by room temperature photoluminescence (PL) spectra. The PL emission from the ZnS nanoparticles shows a sharp peak in the UV region (334 nm) corresponding to the band edge and a broad peak in the visible region which can be attributed to the sulphur vacancies, cation vacancies and surface states in the nanocrystals. The yellow emission from the Mn-doped ZnS nanoparticles can be attributed to the radiative transition between $^4T_1$ and $^6A_1$ levels within the $3d^5$ orbital of Mn^{2+}.

1 Introduction

Synthesis of nanoparticles has been the focus of an ever increasing number of researchers worldwide, mainly due to their unique optical and electronic properties [1–5], which makes them ideal for a wide spectrum of applications ranging from displays and lasers [6, 7] to in vivo biological imaging. A variety of preparation methods have been reported for the synthesis of nanoparticles, such as magnetic liquids [8], metal–polymer nanocomposites [9], semiconductors [10], and colloidal systems [11]. Colloidal nanoparticles have received considerable attention in recent years because of their unique optical, electronic, and magneto-optic properties and consequently their potential applications as optoelectronic devices and biomedical tags. The critical role of dopants in semiconductor devices has stimulated research on the properties and the potential applications of doped semiconductor nanocrystals. Over the past decade, liquid phase pulsed laser ablation (LP-PLA) technique has aroused immense interest [12, 13]. In LP-PLA techniques, laser pulses fall on the target surface through liquids transparent to that wavelength forming cavitation bubbles. When the ablation plume interacts with the surrounding liquid media, which upon their collapse, give rise to extremely high pressure and temperature. These conditions are, however, localized and exist across the nanometer scale. LP-PLA has proven to be an effective method for preparation of many nanostructured materials, including nanocrystalline diamond [14], cubic boron nitride [15], ZnO [16], Ti [17], Ag [18, 19], Au [19–21], TiC [22], ZnO/Au nanocomposites [23], and hydroxyapatite [24].

Efficient phosphors for lighting applications, flat panel displays, sensors, etc,. have always been a goal for researchers. Conventional phosphors are in micrometer scale, so light scattering at grain boundaries is strong and that decreases light output. Nanophosphors can be prepared from tens to hundreds of nanometers that are smaller than the visible wavelength and can reduce scattering, thereby enhancing the luminescence efficiency. Zinc sulfide is a wide band gap ($E_g = 3.6$ eV at 300 K) semiconductor, which is considered important for applications such as ultraviolet-light-emitting diodes, electroluminescent devices, flat panel displays, sensors, and injection lasers [25–29]. Under ambient conditions, ZnS has two types of polymorphs: zinc blende (cubic) and wurtzite (hexagonal). The cubic ZnS is stable at room temperature, whereas the

P. M. Aneesh · M. R. Shijeesh · A. Aravind · M. K. Jayaraj (✉)
Optoelectronic Devices Laboratory, Department of Physics, Cochin University of Science and Technology, Cochin 682 022, India
e-mail: mkj@cusat.ac.in

hexagonal ZnS is stable at temperatures higher than 1,020 °C. When doped with some metal cations (including transition metal ions and rare-earth elements), ZnS is an excellent phosphor exhibiting photoluminescence (PL), electroluminescence (EL), thermoluminescence and triboluminescence [30–34]. Among these elements, Mn doping in ZnS attracts a great deal of interest since Mn doping not only can enhance its optical transition efficiency, but also induce the material to exhibit interesting optical properties [35–38] which is obviously an effective way to enhance the luminescent properties of ZnS for practical applications.

Manzoor et al. [39] reported the growth of Cu^{+}–Al^{3+} and Cu^{+}–Al^{3+}–Mn^{2+} doped ZnS nanoparticles by wet chemical method for electroluminescent applications. The high fluorescent efficiency and dispersion in water make ZnS:Mn nanoparticles an ideal candidate for biological labeling. Since ZnS is an environmentally friendly material; it eliminates the potential toxicity problems. The growth of doped systems of II–VI semiconductor by LP-PLA is not yet reported to our knowledge. Here we report the growth, structural and luminescent characteristics of undoped and Mn-doped ZnS nanoparticles.

2 Experimental details

2.1 Target preparation

The ZnS target was prepared by firing ZnS (99.99 %, Alfa Aesar) powder in H_2S atmosphere at 550 °C for 6 h. ZnS:Mn target with 2 at.% of Mn was synthesized in the laboratory by high temperature (900 °C) solid-state reaction between ZnS (99.99 %, Alfa Aesar) and MnO (99.99 %, Alfa Aesar). ZnS:Mn target of 4-mm thick and diameter 13 mm was obtained after sintering the pressed ZnS:Mn pellet at 550 °C for 6 h in H_2S atmosphere.

2.2 Liquid phase pulsed laser ablation (LP-PLA)

The sintered ZnS and ZnS:Mn target were used for the preparation of nanoparticles by liquid phase pulsed laser ablation. These targets, immersed in 15 mL of distilled water, were ablated at room temperature by the fourth harmonics (266 nm) of a Nd:YAG laser with repetition frequency of 10 Hz and pulse duration of 7 ns. The experimental arrangement is shown in Fig. 1. The spot size of the laser beam falling on the target surface after focusing by a lens of focal length 20 cm was 2 mm and the ablation was carried out at laser energy of 25 mJ/pulse for 1 h. This simple technique produced doped and undoped ZnS nanoparticles, at room temperature, well dispersed in liquid media.

The synthesized targets were characterized for their structure by X-ray diffraction (XRD) (Rigaku D max-C) with Cu K_α radiation. The particle size, distribution, and crystallinity of synthesized nanoparticles were investigated by transmission electron microscopy (JEOL, TEM) operating at an accelerating voltage of 200 kV. The sample for TEM was prepared by placing a drop of the ZnS nanoparticle colloidal solution onto a carbon-coated copper grid. The grids were dried before recording the micrographs. The room temperature PL spectra were recorded using Jobin-Yvon Fluoromax-3 spectrometer equipped with 150 W Xenon lamp.

3 Results and discussion

The crystalline structure of the target was analyzed by XRD with Cu K_α radiation (wavelength = 1.5418 Å). The XRD pattern of undoped and doped ZnS pellet is shown in Fig. 2.

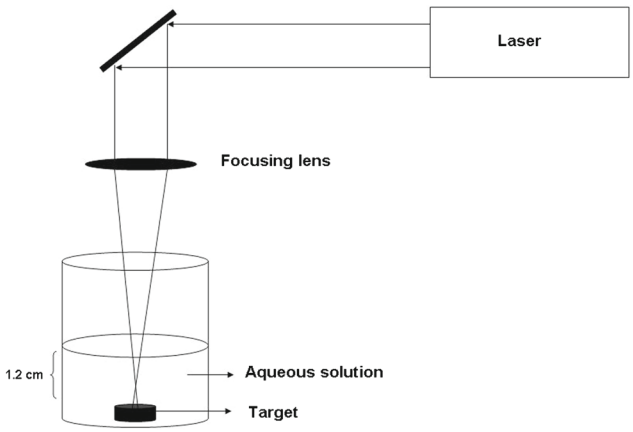

Fig. 1 Experimental setup for the growth of ZnS nanoparticles by LP-PLA

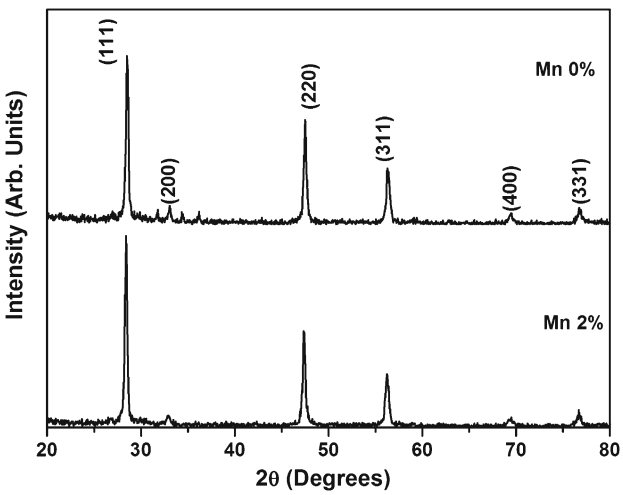

Fig. 2 The XRD pattern of ZnS:Mn target synthesized by solid-state reaction

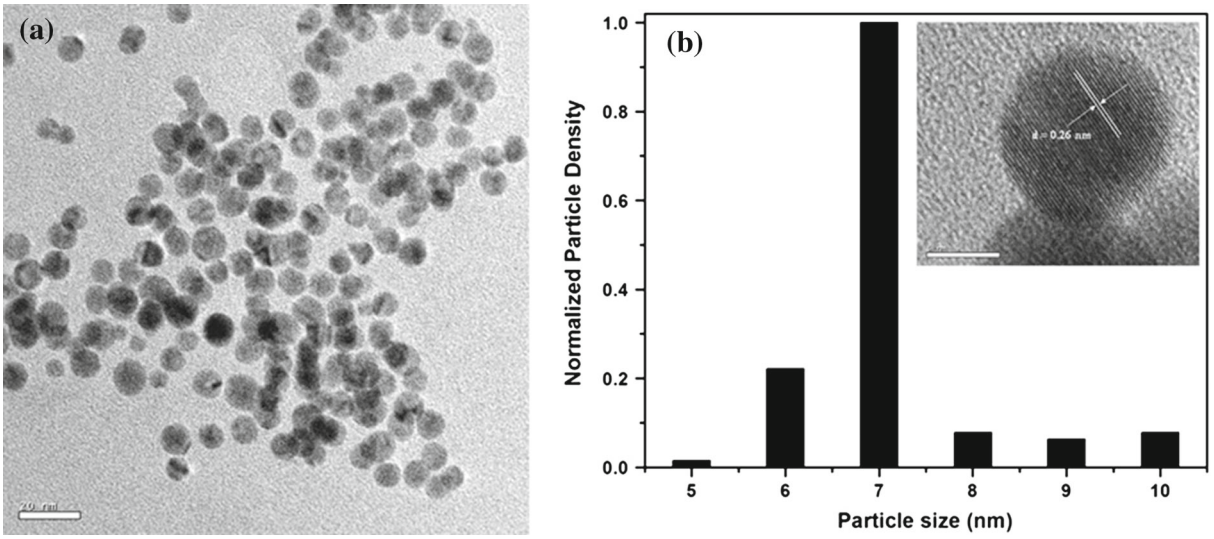

Fig. 3 **a** The TEM image of ZnS nanoparticles in water synthesized by LP-PLA technique. **b** The particle size distribution of ZnS nanoparticles at laser fluence 25 mJ/pulse ablated for 1 h. Inset shows high-resolution TEM image of ZnS nanoparticles

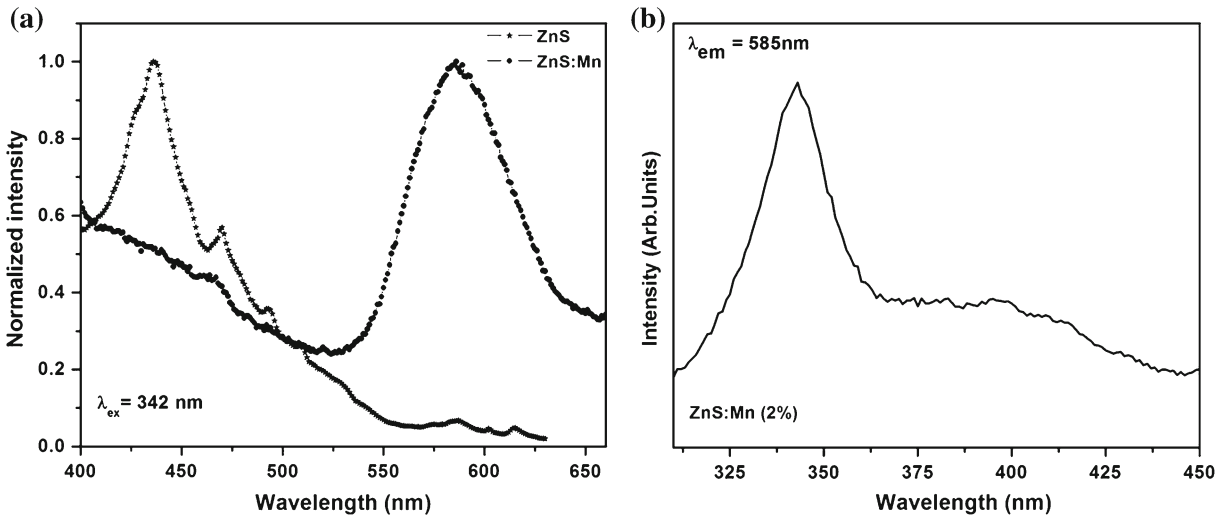

Fig. 4 **a** Room temperature PL emission spectra of ZnS and ZnS:Mn nanoparticles ablated at 25 mJ/pulse for 1 h excited at 342 nm. **b** Room temperature PLE spectra of ZnS:Mn nanoparticles

The XRD pattern shows the cubic structure of ZnS:Mn (0 and 2 at.%) targets. It can be seen that the Mn incorporation has not changed the structure of ZnS. The lattice constant is calculated and for pure ZnS, it is 5.345 nm and for ZnS:Mn is 5.438 nm. The Mn^{2+} ions may have replaced the Zn^{2+} considering the similar ionic radii of Zn (74 pm) and Mn (67 pm) in the ZnS:Mn lattice without any structural change. The successful incorporation of Mn in ZnS host lattice is evident from the increase in lattice constant.

The formation of nanoparticles of undoped ZnS was confirmed by TEM. TEM analysis revealed that the resulting product after laser ablation for 1 h with energy of 25 mJ/pulse in water is spherical in shape and particles are in the nano regime, as shown in Fig. 3a. From TEM analysis, the formation of other molecules or core shell structure was not observed.

Statistical size analysis (Fig. 3b) shows almost uniform particle size distribution with a particle size of 7 nm for ZnS nanoparticles grown at laser fluence 25 mJ/pulse ablated for 1 h. Inset of Fig. 4 shows the high-resolution TEM (HRTEM) images of ZnS nanoparticles showing parallel lines of atoms. The interplanar spacing as obtained from the HRTEM image is 0.26 nm which corresponds to (200) plane of ZnS.

Room temperature PL emission and excitation spectra (PLE) of ZnS and Mn-doped ZnS nanoparticles were investigated in view of luminescent applications. Figure 4a

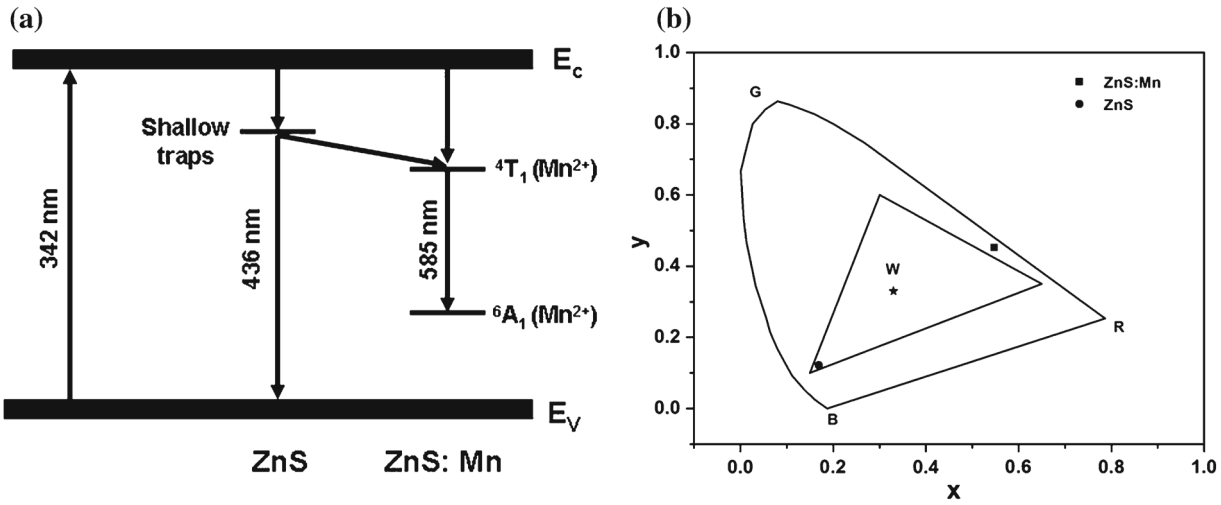

Fig. 5 **a** Simplified energy level diagram of ZnS and Mn-doped ZnS nanoparticles. The energies of absorption and emission lines are also shown. **b** CIE coordinates of PL emission of pure and Mn-doped ZnS nanoparticles

shows the PL emission spectra (on excitation with 342 nm) of ZnS and Mn-doped ZnS nanoparticles ablated at 25 mJ/pulse for 1 h. The emission spectra of ZnS nanoparticles shows a peak at 436 nm. The emission at 436 nm can be attributed to the sulfur vacancy. This agrees with the emission peak observed by Becker and Bard in ZnS phosphor [40].

The ZnS:Mn nanoparticles showed yellow emission at 585 nm. The emission at 585 nm can be attributed to the radiative transition between $^4T_1$ and $^6A_1$ levels within the $3d^5$ orbital of Mn^{2+}, confirming the doping of Mn^{2+} in the ZnS nanostructures [41]. The PL emission spectra of ZnS:Mn does not show any emission corresponding to sulfur vacancy.

As previously discussed in the literature [42], during the doping of Mn^{2+} in the ZnS nanoparticles, Mn^{2+} ions replaces Zn^{2+} in the lattice sites of ZnS host and it occupies the tetrahedral cationic site with T_d symmetry. Upon photo illumination, excitation of electron from valance band of ZnS to the conduction band takes place and it subsequently decays to some surface and defect states by normal recombination process. But during the doping of Mn in ZnS nanoparticles, the electron may be captured by Mn^{2+} ion in the $^4T_1$ level and subsequently decays to $^6A_1$ level radiatively. Thus Mn doping favors the radiative transition between $^4T_1$ and $^6A_1$ levels of manganese by reducing the nonradiative recombinations.

The room temperature PLE spectra of Mn-doped ZnS nanoparticles ($\lambda_{em} = 585$ nm) show the excitation wavelength is 342 nm. Figure 5a shows the schematic representation of the main energy levels identified in the excitation and emission process.

Color characterization of a spectral distribution is done to gauge the quality of its chromaticity. This is accomplished using color coordinates [42]. The Commission Internationale de l'Eclairage (CIE) color coordinates measured from the photoluminescent emission of undoped and Mn-doped ZnS sample were found to be (0.169, 0.122) and (0.544, 0.454), respectively. These coordinates can be represented inside a gamut drawn from the standard x, y values (Fig. 5b). This clearly indicates the purity of the yellow color of the Mn-doped ZnS while the undoped sample shows blue emission.

4 Conclusion

ZnS and ZnS:Mn nanoparticles were prepared by LP-PLA. The targets for LP-PLA were synthesized by the solid-state reaction. The cubic structure of ZnS:Mn (0, 2 at.%) targets was confirmed by XRD. Mn has been successfully incorporated into the ZnS host lattice as evident from the increase in lattice constant. The structural characterization of laser ablated nanoparticles is obtained from the TEM measurements. The TEM analysis confirms the average particle size of the ZnS samples as 7 nm. The PL spectrum of the pure sample shows an emission in the blue region (436 nm) corresponding to the sulfur vacancy for an excitation wavelength of 342 nm. The PL spectra of ZnS:Mn shows a yellow emission at 585 nm under same excitation. This can be attributed to the radiative transition between $^4T_1$ and $^6A_1$ levels within the $3d^5$ orbital of Mn^{2+}. The CIE color coordinates calculated from the PL spectrum confirms the yellow emission of ZnS:Mn nanoparticles. The highly luminescent nature of nanoparticles shows that these nanoparticles are ideal candidates for imaging of tumor cells and living cells and for targeted drug delivery applications.

Acknowledgments This work is supported by the Department of Science and Technology under the Nano Science and Technology Initiative. One of the authors (PMA) thanks Council of Scientific and Industrial Research for the research fellowship award.

References

1. Y. Wu, P. Yang, Chem. Mater. **12**, 605 (2000)
2. M. Morales, C.M. Lieber, Science **279**, 208 (1998)
3. W.S. Shi, Y.F. Zheng, N. Wang, C.S. Lee, S.T. Lee, J. Vac. Sci. Technol. B **19**, 115 (2001)
4. Y. Cui, Q. Wei, H. Park, C.M. Leiber, Science **293**, 1298 (2001)
5. M.H. Huang, S. Mao, H. Feick, H. Yan, Y. Wu, H. Kind, E. Weber, R. Russo, P. Yang, Science **292**, 1897 (2001)
6. J.T. Andrews, P. Sen, J. Appl. Phys. **91**, 2827 (2002)
7. L.V. Asryana, M. Grundmann, N.N. Ledentsov, O. Stier, D. Bimberg, J. Appl. Phys. **90**, 1666 (2001)
8. K.V.P.M. Shafi, S. Wizel, T. Prozorov, A. Gedanken, Thin Solid Films **318**, 38 (1998)
9. S.P. Gubin, J.D. Kosobudskii, Russ. Chem. Rev. **52**, 776 (1983)
10. J. Shi, S. Gilder, K. Babcock, D.D. Awschalom, Science **271**, 937 (1996)
11. Henglein, J. Phys. Chem. **97**, 5457 (1993)
12. G.W. Yang, J.B. Wang, Appl. Phys. A **71**, 343 (2000)
13. C.H. Liang, Y. Shimizu, M. Masuda, T. Sasaki, N. Koshizaki, Chem. Mater. **16**, 963 (2004)
14. S. Kitazawaa, H. Abeb, S. Yamamoto, J. Phys. Chem. Sol. **66**, 555 (2005)
15. J.B. Wang, G.W. Yang, C.Y. Zhang, X.L. Zhong, AZh Ren, Chem. Phys. Lett. **367**, 10 (2003)
16. R.S. Ajimsha, G. Anoop, A. Aravind, M.K. Jayaraj, Electrochem. Solid State Lett. **11**, K14 (2008)
17. O. Yavas, A. Schilling, J. Bischof, J. Boneberg, P. Leiderer, Appl. Phys. A **64**, 331 (1997)
18. G.A. Shafeev, E. Freysz, F. Bozon-Verduraz, Appl. Phys. A **78**, 307 (2004)
19. R. Sreeja, R. Reshmi, P.M. Aneesh, M.K. Jayaraj, Sci. Adv. Mater. **4**, 439 (2012)
20. J.P. Sylvestre, S. Poulin, A.V. Kabashin, E. Sacher, M. Meunier, J.H.T. Luong, J. Phys. Chem. B **108**, 16864 (2004)
21. R. Sreeja, P.M. Aneesh, A. Aravind, R. Reshmi, R. Philip, M.K. Jayaraj, J. Electrochem. Soc. **156**(10), K167 (2009)
22. S.I. Dolgaev, A.V. Simakin, V.V. Voronov, G.A. Shafeev, F. Bozon-Verduraz, Appl. Surf. Sci. **186**, 546 (2002)
23. G. Bajaj, R.K. Soni, Appl. Surf. Sci. **256**, 6399 (2010)
24. K. Hasna, S.S. Kumar, M. Komath, M.R. Varma, M.K. Jayaraj, K.R. Kumar, Phys. Chem. Chem. Phys. (2013). doi:10.1039/c3cp42648c
25. Y.F. Zhu, D.H. Fan, W.Z. Shen, J. Phys. Chem. C **112**, 10402 (2008)
26. Z. Quan, D. Yang, C. Li, D. Kong, P. Yang, Z. Cheng, J. Lin, Langmuir **25**, 10259 (2009)
27. Q. Sun, Y.A. Wang, L. Li, D. Wang, T. Zhu, J. Xu, C. Yang, Y. Li, Nat. Photon **1**, 717 (2007)
28. X. Fang, Y. Bando, M. Liao, U.K. Gautam, C. Zhi, B. Dierre, B. Liu, T. Zhai, T. Sekiguchi, Y. Koide, D. Golberg, Adv. Mater. **21**, 2034 (2009)
29. F. Jain, W. Huang, J. Appl. Phys. **85**, 2706 (1999)
30. B. Dong, L. Cao, G. Su, W. Liu, H. Qu, D. Jiang, J. Colloid, Interface Sci. **339**, 78 (2009)
31. T. Kang, J. Sung, W. Shim, H. Moon, J. Cho, Y. Jo, W. Lee, B. Kim, J. Phys. Chem. C **113**, 5352 (2009)
32. P.A. Jos′e, J.L. Beatriz, C. Eloisa, E. Purificaci′on, P. Fabienne, V. Bruno, S. Cl′ement, J. Mater. Chem. **18**, 5193 (2008)
33. S. Hou, Y. Yuen, H. Mao, J. Wang, Z. Zhu, J. Phys. D Appl. Phys. **42**, 215105 (2009)
34. M.K. Jayaraj, C.P.G. Vallabhan, J. Electrochem. Soc. **138**, 1512 (1991)
35. V. Wood, J.E. Halpert, M.J. Panzer, M.G. Bawendi, V. Bulovic, Nano Lett. **9**, 2367 (2009)
36. S. Kar, S. Biswas, ACS Appl. Mater. Interfaces **1**, 1420 (2009)
37. Y. Fang, S. Chu, H. Chen, P. Kao, I. Chen, C. Hwang, J. Electrochem. Soc. **156**, K55 (2009)
38. T.P. Surkova, V.R. Galakhov, E.Z. Kurmaev, Low Temp. Phys. **35**, 79 (2009)
39. K. Manzoor, S.R. Vadera, N. Kumar, T.R.N. Kutty, Appl. Phys. Lett. **84**, 284 (2004)
40. W.G. Becker, A.J. Bard, J. Phys. Chem. **87**, 4888 (1983)
41. J.F. Suyver, S.F. Wuister, J.J. Kelly, A. Meijerink, Nano Lett. **1**, 429 (2001)
42. R. Maity, K.K. Chattopadhyay, Nanotechnology **15**, 812 (2004)
43. G. Wyszecki, W.S. Stiles, *Color Science: concepts and methods, quantitative data and formulae*, 2nd edn. (John Wiley & Sons Inc., New York, 1982), p. 131